



Effect of Substrate Temperature on Structural and Optical Properties of Au/SiO₂ Nanocomposite Films Prepared by RF Magnetron Sputtering

Ahmed Belahmar, Ali Chouiyakh*

Department of Physics, Renewable Energy and Environment Laboratory, Faculty of Science, Ibn Tofail University, Kenitra, Morocco

Email: *ali_chouiyakh@hotmail.com

How to cite this paper: Belahmar, A. and Chouiyakh, A. (2017) Effect of Substrate Temperature on Structural and Optical Properties of Au/SiO₂ Nanocomposite Films Prepared by RF Magnetron Sputtering. *Open Access Library Journal*, 4: e3810. <https://doi.org/10.4236/oalib.1103810>

Received: July 5, 2017

Accepted: August 18, 2017

Published: August 21, 2017

Copyright © 2017 by authors and Open Access Library Inc.

This work is licensed under the Creative Commons Attribution International License (CC BY 4.0).

<http://creativecommons.org/licenses/by/4.0/>



Open Access

Abstract

Silica films containing gold nanoparticles were grown by magnetron radio frequency (rf) sputtering technique under various deposition conditions. The structural and optical properties of the composite films deposited at 400°C substrate temperature were compared with those deposited at room temperature. Effect of substrate temperature of AuNPs on micro structural properties of the Au/SiO₂ nanocomposite films, such as size, dislocation density (δ), strain (ϵ) and lattice distortion (LD) have been investigated. The face-centered cubic crystalline structure of Au nanoparticles inclusion in the amorphous silica dielectric matrix was confirmed using X-ray diffraction. The average grain size of AuNPs has been found in the range of 0.56 - 0.60 nm and 1.15 - 1.23 nm at 3×10^{-3} mbar and 2×10^{-3} mbar argon pressure respectively. The δ , ϵ , LD values change inversely with the increasing of the substrate temperatures. These composites exhibit the optical features of a semiconductor with direct band gap. The band gap energy of 3.85 eV and 4.1 eV achieved for gold nanoparticles when the substrate temperatures increases from 25°C to 400°C. A peak wavelength of the surface plasmon resonance band absorption (SPR) characteristic of gold nanoparticle was found around 500 nm for the sample deposited at 2×10^{-3} mbar and at 400°C substrate temperature.

Subject Areas

Composite Material, Material Experiment, Nanometer Materials

Keywords

Gold Nanoparticles, Sputtering, Lattice Distortion, Substrate Temperature

1. Introduction

Metal nanoparticles embedded in dielectric matrices in the form of nanocomposite films have gained significant research interest due to their multifunctional properties appropriate for various applications ranging from solar cells to targeted drug delivery [1] [2] [3] [4]. The plasmonic properties of the nanocomposite films mainly depend upon the type of nanoparticles (Au or Ag), their morphology and the dielectric constant of the embedding matrix [5] [6] [7] [8] [9]. One of the most important aspects at the nanoscale is that the noble metals like silver and gold exhibit strong absorption band in visible range. The origin of this absorption is attributed to their collective oscillation of conduction band electron in response to the electrical field of the electromagnetic radiation of light [10] [11]. Silicon dioxide (SiO₂), one of the most abundant materials on earth, has broadly been used in various fields such as passivation layers of electronic devices, protection layers of magnetic or optical discs and anti-reflective coatings because of their excellent chemical stability and optical transmittance with low refractive index [12] [13]. Several dielectric matrices, such as SiO₂ have been utilized to fabricate different multifunctional nanocomposites for different applications [14] [15]. Generally, the main motivation behind the use of an insulating matrix is to maintain the necessary separation between metal nanoparticles, thereby preventing an agglomeration of the metallic nanoparticles. Nanocomposite films consisting of metal particles such as gold embedded in a silica matrix have recently been the subject of many studies [16]-[28]. A large number of methods have been used to obtain AuNPs embedded in SiO₂ films, such ion implantation [29] [30], sol-gel [31], plasma enhanced chemical vapor deposition (PECVD) [32], hybrid techniques combining pulsed-DC sputtering and PECVD, which is used for simultaneous Au sputtering and SiO₂ deposition [18] [19], and RF magnetron sputtering [33]-[38]. The flexibility and easy fabrication of diverse composite films are the advantages of sputtering method. The important factors to influence the formation of AuNPs are the working distance between the target and the substrate, rf-power, sputtering time, the substrate temperature, applied voltage, and working pressure. The purpose of this work is to investigate the influence of substrate temperature on the structural and optical properties of gold/silica composite films grown by RF-magnetron sputtering technique. The as-deposited films were characterized by X-ray diffraction and optical absorption spectroscopy.

2. Experimental Methods

The samples, consisting of gold/silica composite thin films, were prepared by conventional radio-frequency magnetron sputtering method using an Alcatel SCM 650 apparatus. The target consisted of pure (99.99%) metal Au chips on top of a 50 mm diameter silica disc placed 60 mm away from the substrates, is shown **Figure 1**.

Sputter deposition, in a radio frequency (13.56 MHz) machine, has been car-

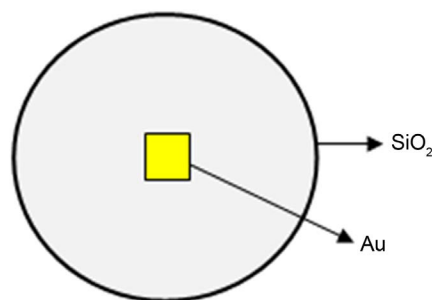


Figure 1. Schematic top view of the target for sputtering of the Au chips and a SiO_2 disc.

ried out after the chamber reached a base pressure of 1×10^{-6} mbar. Deposition was carried out at two argon pressures 2×10^{-3} - 3×10^{-3} mbar and two substrate temperatures 25°C - 400°C . The relevant growth conditions of the films are shown in **Table 1**. Under these conditions, four sets of samples are prepared and they are denoted A_1 (3×10^{-3} mbar, 25°C) A_2 (3×10^{-3} mbar, 400°C) A_3 (2×10^{-3} mbar, 25°C) A_4 (2×10^{-3} mbar, 400°C).

X-ray experiments were performed in a Philips PW 1710 spectrometer using CuK_α radiation ($\lambda = 0.15406$ nm) and a Bragg-Brentano geometry. The diffraction patterns were collected over the range $10^\circ < 2\theta < 80^\circ$ at room temperature. The identification of Au crystalline phases was done using the JCPDS database cards (n_04-0784). Optical absorption spectra, of Au/ SiO_2 composite films, were registered by a Shimadzu UV 30101 PC spectrometer, in near ultra-violet-visible-near infra-red range (NIV-VIS-NIR) from 200 to 2000 nm.

3. Results and Discussion

3.1. Structural Analysis

Figure 2(a) and **Figure 2(b)** presents the XRD patterns of the samples deposited at two working argon pressure 2×10^{-3} , 3×10^{-3} mbar and at two substrate temperatures 25°C , 400°C . X-ray diffractogram of gold thin film with a cubic structure, presented as a reference, is also reported in **Figure 2**. From **Figure 2(a)**, it is evident that there are no Bragg reflections that are clearly visible in the spectra, due to the small AuNPs. Also, it well known that the peak centered on $2\theta = 26^\circ$, in the spectra of all the samples, is attributed to the amorphous silica. It can be expected that the measured spectra of the composite films results from the superposition of two diffractograms, assigned to small gold particles and the amorphous silica matrix. The XRD spectra of the series A_1 and A_2 have the same appearance. The effect of substrate temperature on these two series may be neglected. On the other hand, for the series A_3 and A_4 , the intensity and the full width at half maximum of the diffraction peak corresponding to Au(111) orientation decrease with increase in deposition temperature. This may be due to the improvement in the crystallinity of the AuNPs at higher deposition temperatures and increases the mobility of added atoms which facilitate the grain growth [39].

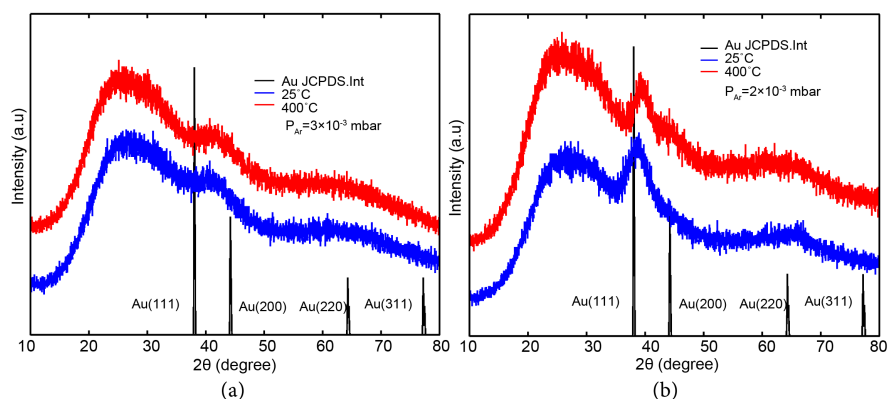


Figure 2. XRD patterns of gold thin films and Au/SiO₂ composite deposited with two Argon pressures, two substrate temperatures.

Table 1. Films growth conditions.

| | |
|-------------------------------|---------------------------------------|
| Working argon pressure (mbar) | $2 \times 10^{-3} - 3 \times 10^{-3}$ |
| Initial pressure(mbar) | 1×10^{-6} |
| Au target (%) | 2.6 |
| Bias (V) | -50 |
| Power (W) | 50 |
| Substrate Temperature | 25°C - 400°C |

As shown in **Figure 2**, it is difficult to determine crystalline phases and size. However, using a commercial software program available on our computer, the XRD patterns were deconvoluted, assuming pseudo-Voigt functions in order to obtain the peak position intensity and the preferential growth of the and full width at half maximum (FWHM). Note that the purpose of the deconvolution is to fit the measured XRD spectrum in well-defined peaks to which a physical meaning can be attributed. For more details see the works [40] [41] [42]. **Figure 3** presents the curve fitting of the XRD spectrum of A_3 serie. Outside the peak assigned to amorphous silica film, the diffraction peaks resulting from the fitting are attributed to the crystal planes of Au(111), Au(200) and Au(220). The peak positions are in agreement with the well known data: JCPDS-04-04784 characteristic of the FCC cubic structure, indicating that the small gold particles should adopt a fcc-like structure. **Table 2** summarizes the fitting parameters determined from the Au(111) orientation plane for all the samples.

The average crystallite size (D) can be estimated from the Debye–Scherrer Equation [43].

$$D = k\lambda / \beta \cos \theta \quad (1)$$

Where, k is the Scherrer constant and is equal to 0.9, θ is the Bragg's angle, λ is the wavelength of the CuK α radiation line and β is the full width at half maximum (FWHM) of peak in radian. The average crystallite size was calculated and it was found in the range between 0.56 nm and 0.6 nm

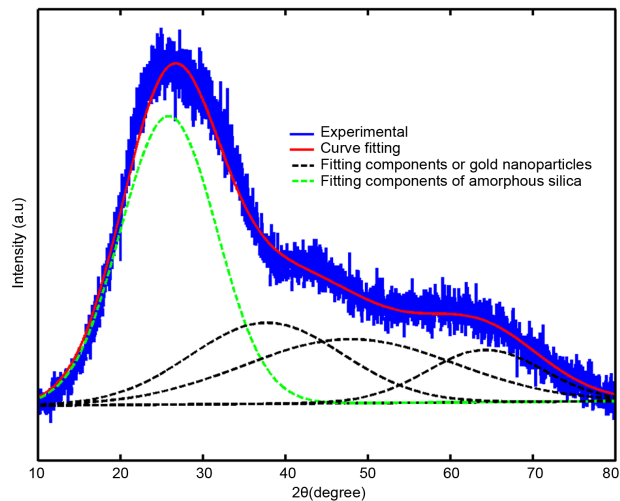


Figure 3. XRD diffraction patterns of A_3 serie and their curve fitting.

Table 2. Results of the curves fitting of the experimental diffractograms of the four series.

| Argon pressure P_{Ar} (mbar) | Sample Number | Substrate Temperature T_s ($^{\circ}C$) | Bragg's angle 2θ (degree) | Particle size D (nm) |
|-----------------------------------|---------------|------------------------------------------------|-------------------------------------|---------------------------|
| 3×10^{-3} | A1 | 25 | 39.82 | 0.56 |
| | A2 | 400 | 39.73 | 0.60 |
| 2×10^{-3} | A3 | 25 | 38.65 | 1.15 |
| | A4 | 400 | 39.55 | 1.23 |

and 1.15 - 1.23 nm at 3×10^{-3} mbar and 2×10^{-3} mbar argon pressure respectively corresponding to prominent (111) peak. The variation of nanoparticle size with respect to substrate temperature is presented in **Table 2**. It is observed that the grain size increases with an increase of substrate temperature. Also, the larger grain sizes were obtained with lower argon pressure deposition.

From XRD results, the various structural parameters like dislocation density (δ), strain (ε) and lattice distortion (LD), which are commonly used to describe the structural analysis, were calculated using the following equations and evaluated data are presented in **Table 3** [44].

$$\delta = 1/D^2 \quad (2)$$

$$\varepsilon = \beta \cos \theta / 4 \quad (3)$$

$$LD = \beta / 4 \tan \theta \quad (4)$$

where, D is crystalline size, β is full-width at half maximum in radians, θ is the Bragg's angle.

Table 3 demonstrates that the strain and dislocation density of the material of the film decrease with an increase of substrate temperature. This may due to the increase in grain size [45]. Further, the decrease in strain indicates a decrease of lattice constant with an increase of substrate temperature [46].

3.2. Optical Studies

Figure 4 presents the measured optical transmission spectra of all the samples. It is observed that the transmittance increases in the visible range and small increasing of the transmittance maxima for wavelength larger than 1200 nm, when the substrate temperature changes from 25°C to 400°C for A_3 and A_4 series. No significant change was observed in the case of A_1 and A_2 series. This observation is confirmed by the obtained from XRD measurements. Moreover, the transmittance curves denote a pronounced blue-shift of the absorption edge with the enhancement of substrate temperature. The Blue-shift in the absorption edge is ascribed to an enlargement of the optical band gap suggesting a strong effect of the size AuNPs on the electronic properties. Therefore, the position of the absorption edge can be controlled in both the near UV and whole visible band. Moreover, from the optical transmittance measurements we may calculate the absorption coefficient, α , of the films using the formula:

$$\alpha = \frac{\ln(100/T)}{d} \quad (5)$$

where T , is the transmittance and d , is the film thickness.

From the absorbance curves presented in **Figure 5**, we note the absence of the typical SPR extinction peaks, in the A1, A2 and A3 series. This is an indication that the AuNPs should be incorporated in silica films with size lower than 2 nm. For the A4 series, Surface plasmon resonance broad absorption peak is observed

Table 3. Micro structural parameters of the series A1, A2, A3 and A4.

| Sample Number | Dislocation density (lines/m ²) (δ) $\times 10^{16}$ | Strain (ε) $\times 10^{-2}$ | Lattice distortion (LD) $\times 10^{-2}$ |
|---------------|------------------------------------------------------------------------------|----------------------------------------------|---------------------------------------------|
| A1 | 318.88 | 6.44 | 1.92 |
| A2 | 277.78 | 6.01 | 1.27 |
| A3 | 75.61 | 3.14 | 1.12 |
| A4 | 66.10 | 2.94 | 1.00 |

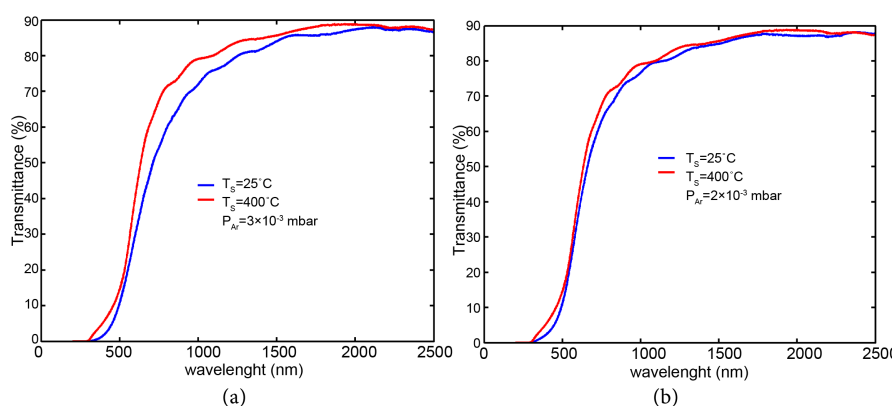


Figure 4. Transmittance spectra of Au/SiO₂ nanocomposite films sputtered at two substrate temperatures and argon pressures: (a) at 3×10^{-3} mbar; (b) at 2×10^{-3} mbar.

in the absorption spectra around 500 nm. These results suggest that Au/SiO₂ samples have a semi-conductor character.

According to the Tauc relation, the absorption coefficient α for direct band gap material is given by [47],

$$(\alpha h\nu)^2 = A(h\nu - E_g) \quad (6)$$

where A is a constant, E_g is the optical gap expressed in eV and $h\nu$ is the photon energy in eV. Figure 6 shows the plot of $(\alpha h\nu)^2$ vs. the photon energy ($h\nu$) of the Au/SiO₂ nanocomposite thin films with different substrate temperature and argon pressures. The (E_g) deduce values of A1 and A2 series varied from 3.9 eV to 4.07 eV, while the (E_g) values of A3 and A4 varied from 3.85 eV from 4.1 eV when the substrate temperature increases from 25°C to 400°C.

The obtained nanocomposite materials have lower absorbance and higher transmittance in the visible region can be used as a suitable antireflection layer in solar cells working mainly in the visible region [48].

4. Conclusion

Au/SiO₂ nanocomposite films have been prepared by RF-sputtering technique.

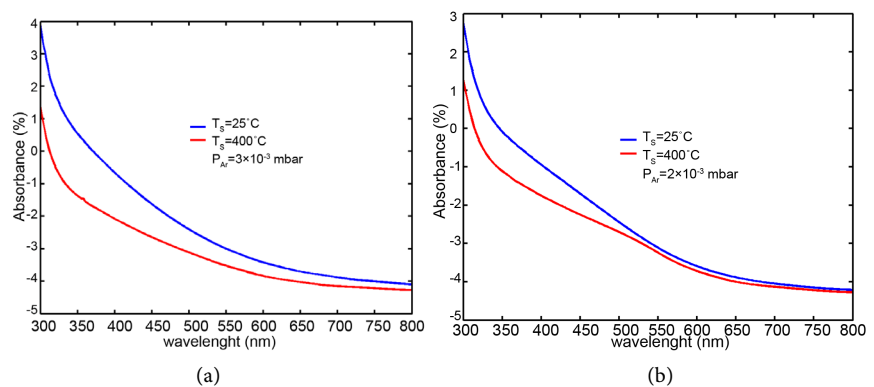


Figure 5. Optical absorption spectra of Au/SiO₂ nanocomposite films sputtered at two substrate temperatures and argon pressures: (a) at 3×10^{-3} mbar; (b) at 2×10^{-3} mbar.

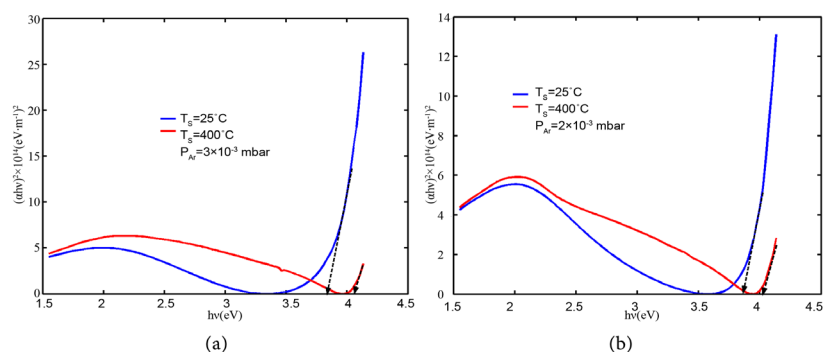


Figure 6. Plot of $(\alpha h\nu)^2$ versus photon energy $h\nu$ for Au/SiO₂ deposited at two substrate temperatures and argon pressures: (a) at 3×10^{-3} mbar; (b) at 2×10^{-3} mbar.

The effect of argon pressure and substrate temperature on the structural and optical properties of the composite films was investigated. XRD analysis shows that the size of the Au NPs increases, the strain, lattice distortion and dislocation density decrease with the increasing the substrate temperature. The transmittance measurements were taken at room temperature in the wavelength range 200 - 2000 nm. The absorption coefficient and optical gap energy were deduced from the transmittance measurements. The increasing of the substrate temperature increases the optical gap energy. The best transparency of composite thin films is obtained at low argon pressure and at higher substrate temperature. These results can give a design guide how to control the properties of composite films by metal nanoparticles.

Acknowledgements

We are grateful to Professor M.J.M. Gomes from the Centre of Physics, University of Minho, Portugal, for the experimental support.

References

- [1] Jain, P.K., Huang, X.H., El-Sayed, I.H. and El-Sayed, M.A. (2008) Noble Metals on the Nanoscale: Optical and Photo-Thermal Properties and Some Applications in Imaging, Sensing, Biology, and Medicine. *Accounts of Chemical Research*, **41**, 1578-1586. <https://doi.org/10.1021/ar7002804>
- [2] Jamali, M., Hedayati, M.K., Mozooni, B., Javaherirahim, M., Abdelaziz, R., Zillohu, A.U. and Elbahri, M. (2010) Photoresponsive Transparent Conductive Metal with a Photobleaching Nose. *Advanced Materials*, **23**, 4243-4247. <https://doi.org/10.1002/adma.201102353>
- [3] Atwater, H.A. and Polman, A. (2010) Plasmonics for Improved Photovoltaic Devices. *Nature Materials*, **9**, 205-213. <https://doi.org/10.1038/nmat2629>
- [4] Elbahri, M., Hedayati, M.K., Chakravadhanula, V.S.K., Jamali, M., Strunskus, T., Zaporotchenko, V. and Faupel, F. (1997) An Omnidirectional Transparent Conducting-Metal-Based Plasmonic Nanocomposite. *Advanced Materials*, **23**, 1993. <https://doi.org/10.1002/adma.201003811>
- [5] Kelly, K.L., Coronado, E., Zhao, L.L. and Schatz, G.C. (2003) The Optical Properties of Metal Nanoparticles: The Influence of Size, Shape, and Dielectric Environment. *The Journal of Physical Chemistry B*, **107**, 668-677. <https://doi.org/10.1021/jp026731y>
- [6] Miller, M.M. and Lazarides, A.A. (2005) Sensitivity of Metal Nanoparticle Surface Plasmon Resonance to the Dielectric Environment. *The Journal of Physical Chemistry B*, **109**, 21556-21565. <https://doi.org/10.1021/jp054227y>
- [7] Dalacu, D. and Martinu, L. (2000) Spectroellipsometric Characterization of Plasma-Deposited Au/SiO₂ Nanocomposite Films. *Journal of Applied Physics*, **87**, 228-235. <https://doi.org/10.1063/1.371849>
- [8] Noguez, C. (2007) Surface Plasmons on Metal Nanoparticles: The Influence of Shape and Physical Environment. *The Journal of Physical Chemistry C*, **111**, 3806-3819. <https://doi.org/10.1021/jp066539m>
- [9] Link, S. and EL-Sayed, M.A. (2000) Shape and Size Dependence of Radiative, Non-Radiative and Photothermal Properties of Gold Nanocrystals. *International Reviews*

- in Physical Chemistry*, **19**, 409-453. <https://doi.org/10.1080/01442350050034180>
- [10] Kreibig, U. and Vollmer, M. (1995) Optical Properties of Metal Clusters. Springer, Berlin. <https://doi.org/10.1007/978-3-662-09109-8>
- [11] Bohren, C.F. and Huffman, D.R. (1983) Absorption and Scattering of Light by Small Particles. Wiley Interscience, New York.
- [12] Toki, K., Kusakabe, K., Odani, T., Kobuna, S. and Shimizu, Y. (1996) Deposition of SiO₂ and Ta₂O₅ Films by Electron-Beam-Excited Plasma Ion Plating. *Thin Solid Films*, **281-282**, 401-403.
- [13] Oyama, T., Ohsaki, H., Tachibana, Y., Hayashi, Y., Ono, Y. and Horie, N. (1999) A New Layer System of Anti-Reflective Coating for Cathode Ray Tubes. *Thin Solid Films*, **351**, 235-240.
- [14] Mohapatra, S., Mishra, Y.K., Avasthi, D.K., Kabiraj, D., Ghatak, J. and Varma, S. (2007) Synthesis of Au Nanoparticles in Partially Oxidized Si Matrix by Atom Beam Sputtering. *Journal of Physics D: Applied Physics*, **40**, 7063-7068. <https://doi.org/10.1088/0022-3727/40/22/030>
- [15] Takele, H., Greve, H., Pochstein, C., Zaporozhchenko, V. and Faupel, F. (2006) Plasmonic Properties of Ag Nanoclusters in Various Polymer Matrices. *Nanotechnology*, **17**, 3499-3505. <https://doi.org/10.1088/0957-4484/17/14/023>
- [16] Liao, H.B., Xiao, R.F., Fu, J.S., Yu, P., Wong, G.K. and Sheng, P. (1997) Large Third-Order Optical Nonlinearity in Au: SiO₂ Composite Films near the Percolation Threshold. *Applied Physics Letters*, **70**, 1-3. <https://doi.org/10.1063/1.119291>
- [17] Tanahashi, I., Manabe, Y., Tohda, T., Sasaki, S. and Nakamura, A. (1996) Optical Nonlinearities of Au/SiO₂ Composite Thin Films Prepared by a Sputtering Method. *Journal of Applied Physics*, **79**, 1244-1249. <https://doi.org/10.1063/1.361018>
- [18] Dalacu, D. and Martinu, L. (2000) Temperature Dependence of the Surface Plasmon Resonance in Au/SiO₂ Films. *Applied Physics Letters*, **77**, 4283-4285. <https://doi.org/10.1063/1.1334362>
- [19] Kerboua, C.H., Lamarre, J.M., Martinu, L. and Roorda, S. (2007) Deformation, Alignment and Anisotropic Optical Properties of Gold Nanoparticles Embedded in Silica. *Nuclear Instruments and Methods in Physics Research Section B: Beam Interactions with Materials and Atoms*, **257**, 42-46.
- [20] Lamarre, J.M., Yu, Z., Harkati, C., Roorda, S. and Martinu, L. (2005) Optical and Microstructural Properties of Nanocomposite Au/SiO₂ Films Containing Particles Deformed by Heavy Ion Irradiation. *Thin Solid Films*, **479**, 232-237.
- [21] Belahmar, A. and Chouiyakh, A. (2013) Effect of Post-Annealing on Structural and Optical Properties of Gold Nanoparticles Embedded in Silica Films Grown by RF-Sputtering. *Advances in Physics Theories*, **15**, 38-46.
- [22] Jung, K.H., Yoon, J.W., Koshizaki, N. and Kwon, Y.S. (2008) Fabrication and Characterization of Au/SiO₂ Nanocomposite Films Grown by Radio-Frequency Co-Sputtering. *Current Applied Physics*, **8**, 761-765.
- [23] Yu, G.Q., Tay, B.K., Zhao, Z.W., Sun, X.W. and Fu, Y.Q. (2005) Ion Beam Co-Sputtering Deposition of Au/SiO₂ Nanocomposites. *Physica E: Low-Dimensional Systems and Nanostructures*, **27**, 362-368.
- [24] Zhuo, B., Li, Y., Teng, S. and Yang, A. (2010) Fabrication and Characterization of Au/SiO₂ Nanocomposite Films. *Applied Surface Science*, **256**, 3305-3308.
- [25] Sangpour, P., Akhavan, O., Moshfegh, A.Z. and Roozbehi, M. (2007) Formation of Gold Nanoparticles in Heat-Treated Reactive Co-Sputtered Au-SiO₂ Thin Films. *Applied Surface Science*, **254**, 286-290.

- [26] Cho, S., Lim, H., Lee, K.S., Lee, T.S., Cheong, B., Kim, W.M. and Lee, S. (2005) Spectro-Ellipsometric Studies of Au/SiO₂ Nanocomposite Films. *Thin Solid Films*, **475**, 133-138.
- [27] Kennedy, M.S., Moody, N.R., Adams, D.P., Clift, M. and Bahr, D.F. (2008) Environmental Influence on Interface Interactions and Adhesion of Au/SiO₂. *Materials Science and Engineering: A*, **493**, 299-304.
- [28] Ruffino, F., Grimaldi, M.G., Bongiorno, C., Giannazzo, F., Roccaforte, F. and Raineri, V. (2008) Microstructure of Au Nanoclusters Formed in and on SiO₂. *Superlattices and Microstructures*, **44**, 588-598.
- [29] Takahiro, K., Oizumi, S., Morimoto, K., Kawatsura, K., Isshiki, T., Nishio, K., Nagata, S., Yamamoto, S., Narumi, K. and Naramoto, H. (2009) Application of X-Ray Photoelectron Spectroscopy to Characterization of Au Nanoparticles Formed by Ion Implantation into SiO₂. *Applied Surface Science*, **256**, 1061-1064.
- [30] Cesca, T., Maurizio, C., Kalinic, B., Scian, C., Trave, E., Battaglin, G., Mazzoldi, P. and Mattei, G. (2014) Luminescent Ultra-Small Gold Nanoparticles Obtained by Ion Implantation in Silica. *Nuclear Instruments and Methods in Physics Research Section B: Beam Interactions with Materials and Atoms*, **326**, 7-10.
- [31] Ferrara, M.C., Mirengi, L., Mevoli, A. and Tapfer, L. (2008) Synthesis and Characterization of Sol-Gel Silica Films Doped with Size-Selected Gold Nanoparticles. *Nanotechnology*, **19**, 65706-65714. <https://doi.org/10.1088/0957-4484/19/36/365706>
- [32] Ruffino, F., Bongiorno, C., Giannazzo, F., Roccaforte, F., Raineri, V. and Grimaldi, M.G. (2007) Effect of Surrounding Environment on Atomic Structure and Equilibrium Shape of Growing Nanocrystals: Gold in/on SiO₂. *Nanoscale Research Letters*, **2**, 240-247. <https://doi.org/10.1007/s11671-007-9058-4>
- [33] Liao, H.B., Weijia, W. and Wong, G.K.L. (2003) Preparation and Optical Characterization of Au/SiO₂ Composite Films with Multilayer Structure. *Journal of Applied Physics*, **93**, 4485-4488. <https://doi.org/10.1063/1.1560569>
- [34] Debrus, S., Lafait, J., May, M., Pincon, N., Prot, D., Sella, C. and Venturini, J. (2000) Z-Scan Determination of the Third-Order Optical Nonlinearity of Gold: Silica Nanocomposites. *Journal of Applied Physics*, **88**, 4469-4475. <https://doi.org/10.1063/1.1290260>
- [35] Pinçon, N., Palpant, B., Prot, D., Charron, E. and Debrus, S. (2002) Third-Order Nonlinear Optical Response of Au: SiO₂ Thin Films: Influence of Gold Nanoparticle Concentration and Morphologic Parameters. *The European Physical Journal D-Atomic, Molecular, Optical and Plasma Physics*, **19**, 395-402.
- [36] Belahmar, A. and Chouiyakh, A. (2016) Investigation of Surface Plasmon Resonance and Optical Band Gap Energy in Gold/Silica Composite Films Prepared by RF-Sputtering. *Journal of Nanoscience and Technology*, **2**, 81-84.
- [37] Belahmar, A. and Chouiyakh, A. (2016) Structural and Optical Study of Au Nanoparticles Incorporated in Al₂O₃ and SiO₂ Thin Films Grown by RF-Sputtering. *International Journal of Advanced Research in Computer Science and Software Engineering*, **6**, 109-116.
- [38] Belahmar, A. and Chouiyakh, A. (2016) Influence of Argon Pressure on the Optical Band Gap Energy and Urbach Tail of Sputtered Au/SiO₂ Nanocomposite Films. *International Journal of Advanced Research in Computer Science and Software Engineering*, **6**, 7-13.
- [39] Bhattacharyya, S.R. and Pal, A.K. (2008) Electrical and Optical Properties of Silicon-Doped Gallium Nitride Polycrystalline Films. *Bulletin of Materials Science*, **31**, 73-82. <https://doi.org/10.1007/s12034-008-0013-5>

- [40] Belahmar, A. and Chouiyakh, A. (2014) Influence of the Fabrication Conditions on the Formation and Properties of Gold Nanoparticles in Alumina Matrix Produced by Co-Sputtering. *International Journal of Nano and Material Sciences*, **3**, 16-29.
- [41] Belahmar, A. and Chouiyakh, A. (2016) Sputtering Synthesis and Thermal Annealing Effect on Gold Nanoparticles in Al₂O₃ Matrix. *Journal of Nanoscience and Technology*, **2**, 100-103.
- [42] Belahmar, A. and Chouiyakh, A. (2017) Size and Concentration Effects on Surface Plasmon Resonance and Maxwell-Garnett Absorption in RF-Magnetron Sputtered Au/Al₂O₃ Nanocomposite Films. *Journal of Thin Films Research*, **1**, 1-6.
- [43] Cullity, B.D. and Stock, S.R. (2001) Elements of X-Ray Diffraction. 3rd Edition, Prentice Hall, New York.
- [44] Bindu, B. and Thomas, S. (2014) Estimation of Lattice Strain in ZnO Nanoparticles: X-Ray Peak Profile Analysis. *Journal of Theoretical and Applied Physics*, **8**, 123-134. <https://doi.org/10.1007/s40094-014-0141-9>
- [45] Rakhesh, V. and Vaidyan, V.K. (2009) Effect of Substrate Temperature and Post Deposited Annealing on the Electrical and Photoluminescence Characteristics of Zinc Oxide Films Deposited by Spray Pyrolysis. *Journal of Optoelectronics and Biomedical Materials*, **1**, 281-290.
- [46] Jassim, S.A.J., Zumaila, A.A.R.A. and Al Waly, G.A.A. (2013) Influence of Substrate Temperature on the Structural, Optical and Electrical Properties of CdS Thin Films Deposited by Thermal Evaporation. *Results in Physics*, **3**, 173-178.
- [47] Tauc, J. (1974) Amorphous and Liquid Semiconductors. Plenum, London. <https://doi.org/10.1007/978-1-4615-8705-7>
- [48] Bedia, A., Bedia, F.Z., Aillerie, M., Maloufi, N. and Benyoucef, B. (2015) Morphological and Optical Properties of ZnO Thin Films Prepared by Spray Pyrolysis on Glass Substrates at Various Temperatures for Integration in Solar Cell. *Energy Procedia*, **74**, 529-538.



Open Access Library

Submit or recommend next manuscript to OALib Journal and we will provide best service for you:

- Publication frequency: Monthly
- 9 [subject areas](#) of science, technology and medicine
- Fair and rigorous peer-review system
- Fast publication process
- Article promotion in various social networking sites (LinkedIn, Facebook, Twitter, etc.)
- Maximum dissemination of your research work

Submit Your Paper Online: [Click Here to Submit](#)

Or Contact service@oalib.com